

## Dynamics of a ring of three coupled relaxation oscillators

J. Bridge<sup>a</sup>, L. Mendelowitz<sup>b</sup>, R. Rand<sup>c,\*</sup>, S. Sah<sup>d</sup>, A. Verdugo<sup>e</sup>

<sup>a</sup> Department of Mechanical Engineering, University of the West Indies, St. Augustine, Trinidad

<sup>b</sup> College of Engineering, Cornell University, Ithaca, NY, United States

<sup>c</sup> Department of Theoretical and Applied Mechanics, 207 Kimball Hall, Cornell University, Ithaca, NY 14853-1503, United States

<sup>d</sup> Faculty of Sciences Ain Chock, BP 5366 Maârif, Casablanca, Morocco

<sup>e</sup> Center for Applied Mathematics, Cornell University, Ithaca, NY, United States

### ARTICLE INFO

#### Article history:

Received 20 May 2008

Accepted 21 May 2008

Available online 7 July 2008

#### PACS:

05.45.–a

43.40.Ga

47.20.Ky

#### Keywords:

Coupled oscillators

Nonlinear vibrations

Bifurcations

Perturbations

### ABSTRACT

The dynamics of a ring of three identical relaxation oscillators is shown to exhibit a variety of periodic motions, including clockwise and counter-clockwise wave-like modes, and a synchronous mode in which all three oscillators are in phase. The model involves individual oscillators which exhibit sudden jumps, modeling the relaxation oscillations of van der Pol oscillators. Methods include (i) numerical integration, (ii) a semi-analytical method involving solving transcendental equations numerically, and (iii) perturbation methods. A variety of bifurcations of the periodic motions are identified. This work is motivated by application to the design of a decision-making machine which can sort initial conditions according to their steady state.

© 2008 Elsevier B.V. All rights reserved.

## 1. Introduction

This work concerns the dynamics of a ring of three limit cycle oscillators. Our interest in this system stems from applications to artificial intelligence. The idea is that in any dynamical system in which there are multiple stable steady states, the space of initial conditions may be decomposed into separate basins of attraction, each one corresponding to a different steady state. Thus a given initial condition can be associated with a particular steady state, and a machine which possesses these dynamics can exhibit associative memory, a characteristic property of brain models [1]. Such machines are made possible through the use of MEMS/NEMS technology. Zhalutdinov et al. [2] treated a system of 400 NEMS oscillators and showed how the steady state dynamics were affected by changes in parameters, including coupling strength. Rand and Wong [3] studied a system of four coupled phase-only oscillators and showed that if some of the coupling coefficients were chosen to be negative (called “inhibitory” coupling in the biological literature, [4]) the system could exhibit a continuum of stable steady states.

Limit cycle oscillations are often classified as being either of the sinusoidal type or of the relaxation type. For example in the case of the van der Pol oscillator,

$$\ddot{x} + x - \epsilon(1 - x^2)\dot{x} = 0 \quad (1)$$

\* Corresponding author. Fax: +1 607 255 2011.

E-mail address: [rhr2@cornell.edu](mailto:rhr2@cornell.edu) (R. Rand).

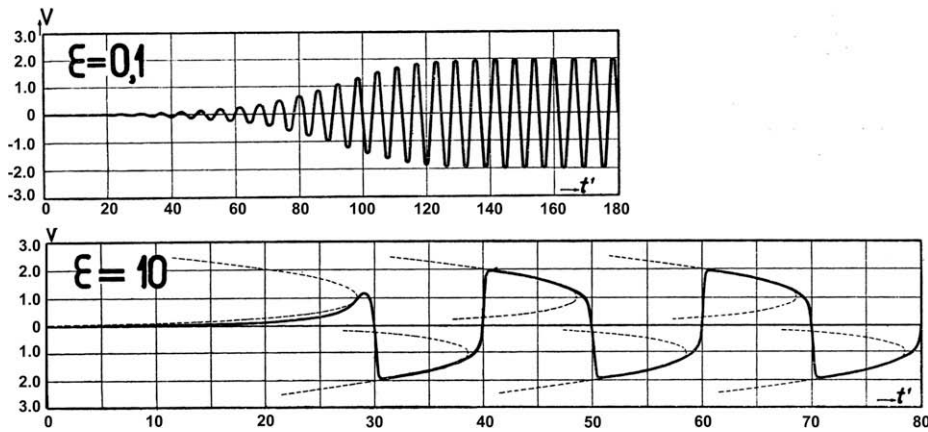


Fig. 1. Solutions of van der Pol's Eq. (1) from his original 1926 paper [5].  $\epsilon = 0.1$  gives a sinusoidal oscillation, while  $\epsilon = 10$  gives a relaxation oscillation.

sinusoidal oscillations result for small values of  $\epsilon$  (say  $0 < \epsilon < 0.1$ ), while relaxation oscillations occur for large values of  $\epsilon$  (say  $\epsilon > 10$ ). See Fig. 1. (For intermediate values of  $\epsilon$  (say  $\epsilon \approx 1$ ), the resulting limit cycle oscillation is neither of sinusoidal nor of relaxation type.)

In a recent paper, Mendelowitz, Verdugo and Rand [6] presented an analysis of a ring of three coupled *sinusoidal* limit cycle oscillators. The purpose of the present work is to extend the work in [6] by considering a ring of three coupled *relaxation* limit cycle oscillators. Because the present work is closely related to that in [6], we therefore present a brief summary of the relevant results obtained in [6]. See Fig. 2 which displays the configuration of three oscillators studied in both [6] as well as in the present work. Modeling each oscillator as a van de Pol oscillator (1), the equations of motion become:

$$\ddot{x} + x - \epsilon(1 - x^2)\dot{x} = -2\epsilon\alpha\dot{z} \tag{2}$$

$$\ddot{y} + y - \epsilon(1 - y^2)\dot{y} = -2\epsilon\alpha\dot{x} \tag{3}$$

$$\ddot{z} + z - \epsilon(1 - z^2)\dot{z} = -2\epsilon\alpha\dot{y} \tag{4}$$

Here each of the oscillators has the same  $\epsilon = 0$  frequency of unity, and  $\alpha > 0$  is a coupling coefficient. In [6] it was found that in the small  $\epsilon$  limit there were three distinct types of sinusoidal periodic motions: a clockwise (CW) mode, a counter-clockwise (CCW) mode, and an in-phase (IP) mode. Each of these modes was characterized by each oscillator performing a nearly sinusoidal motion. The difference between the modes consisted of there being different phase lags between the  $x$ ,  $y$  and  $z$  motions. In the case of the CW and CCW modes, the phases differed by  $120^\circ$  (occurring in the order  $x$ - $y$ - $z$  for CW and  $z$ - $y$ - $x$  for CCW), whereas for the IP mode the phase lags were all zero. It was found that the IP mode did not exist for  $\alpha > 1/2$ , and that it was unstable for  $0 < \alpha < 1/2$ . Both the CW and CCW modes were found to be stable for  $\alpha > 0$ . Regarding the frequencies of these motions, it was found that the CW mode has frequency  $1 - \frac{\sqrt{3}}{2}\epsilon\alpha + O(\epsilon^2)$  whereas the CCW mode has frequency  $1 + \frac{\sqrt{3}}{2}\epsilon\alpha + O(\epsilon^2)$ . The IP mode has frequency  $1 + O(\epsilon^2)$ . In addition to these results, numerical integration was used to obtain an approximation of another mode which was the basin boundary between the regions of attraction of the stable CW and CCW modes. This mode was found to be unstable and of the clockwise variety, although the wave shape was not sinusoidal.

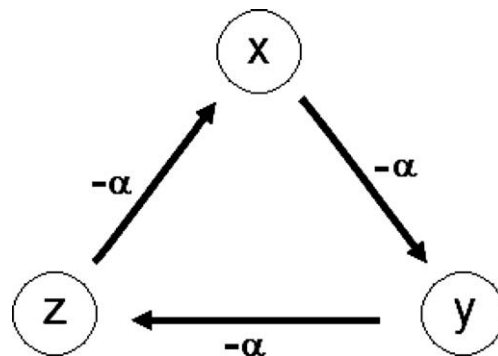


Fig. 2. Schematic diagram of three coupled oscillators which are cyclically coupled. The negative coupling coefficient implies “inhibitory” coupling [4]. See Eqs. (2)–(4) and Eqs. (5)–(7).

## 2. Model

In the case of nearly sinusoidal oscillations (small  $\epsilon$ ), the system of coupled van der Pol oscillators (2)–(4) can be treated by standard perturbation methods such as multiple scales or averaging [6]. However, in the case of relaxation oscillations, the large  $\epsilon$  asymptotics for these same equations involves matched asymptotic expansions with boundary layers occurring in the neighborhood of the relaxation jumps [7,8]. For a system of two coupled van der Pol oscillators, Storti and Rand [9] showed that the stability of the in-phase and out-of-phase modes could be studied by looking for a solution to the first variational equations in the form of matched asymptotic expansions. However they also studied an alternative approach [10,11] which replaced the regions of rapid change in a relaxation oscillation by jumps. It is this approach which uses jumps to model relaxation oscillations which we shall use in the present paper.

We thus propose the following model in which a single uncoupled limit cycle oscillator  $x$  is modeled by a slow phase in which  $x$  slowly decreases from  $x = 2$  to  $x = 1$ , then jumps from  $x = 1$  to  $x = -2$ , then repeats the process with signs reversed, slowly increasing from  $x = -2$  to  $x = -1$ , then jumping from  $x = -1$  to  $x = 2$ . See Fig. 3.

Following [10], we model the slow phases by the simple equation  $x' = -x/2$ , where primes represent differentiation with respect to  $\hat{t} = t/\epsilon$ . For convenience in what follows, we drop the hats  $\hat{\cdot}$  on  $t$ . Thus we are led to the following alternative to the system (2)–(4):

$$\dot{x} + x/2 = -\alpha z \tag{5}$$

$$\dot{y} + y/2 = -\alpha x \tag{6}$$

$$\dot{z} + z/2 = -\alpha y \tag{7}$$

Eqs. (5)–(7) may be more conveniently written in the form:

$$\dot{x} = -\frac{1}{2(1 + \alpha^3)}(x + \alpha^2 y - \alpha z) \tag{8}$$

$$\dot{y} = -\frac{1}{2(1 + \alpha^3)}(y + \alpha^2 z - \alpha x) \tag{9}$$

$$\dot{z} = -\frac{1}{2(1 + \alpha^3)}(z + \alpha^2 x - \alpha y) \tag{10}$$

where it is to be understood that each of  $x, y$  and  $z$  independently jump  $\pm 1$  to  $\mp 2$ . Note that the model assumes that when one of the oscillators jumps, there is no change in position of the other two oscillators. We make the further assumption that all initial conditions satisfy the constraints that  $|x| > 1, |y| > 1$  and  $|z| > 1$ , i.e., we omit motions that lie in the region  $R: \{|x| < 1\} \cup \{|y| < 1\} \cup \{|z| < 1\}$ . The reason for this assumption is that for the single oscillator shown in Fig. 3, the equation  $x' = -x/2$  implies that motions starting in the region  $|x| < 1$  decay to zero, whereas in the van der Pol oscillator (1), such motions would approach the limit cycle since the origin is unstable. Thus we omit region  $R$  in which the model does not accurately represent the limit cycle oscillators (2)–(4).

This work is related to the work of other researchers. In the case of a single oscillator driven by a periodic forcer, a model similar to that of Fig. 3 has been used in [12,13]. In the case of coupled oscillators, the model used in this paper can be contrasted with the approaches in [14–16]. In [14,15], fast threshold modulation is utilized to study the change in position of all oscillators as a result of a jump in one of them. In [16], Malkin’s theorem is used to obtain phase equations for a system of weakly coupled relaxation oscillators.

## 3. Numerical simulation

We begin our discussion of Eqs. (8)–(10) by numerically integrating these equations and displaying a variety of periodic solutions. Fig. 4 shows six different periodic solutions, each obtained by numerical integration for  $\alpha = 0.1$ . For brevity we will refer to these motions by the following abbreviations:

- IP in-phase mode
- CCW counter-clockwise mode with evenly spaced jumps ordered  $y-x-z$
- CW clockwise mode with evenly spaced jumps ordered  $x-y-z$

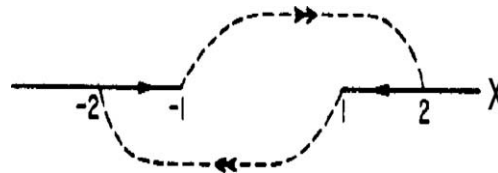
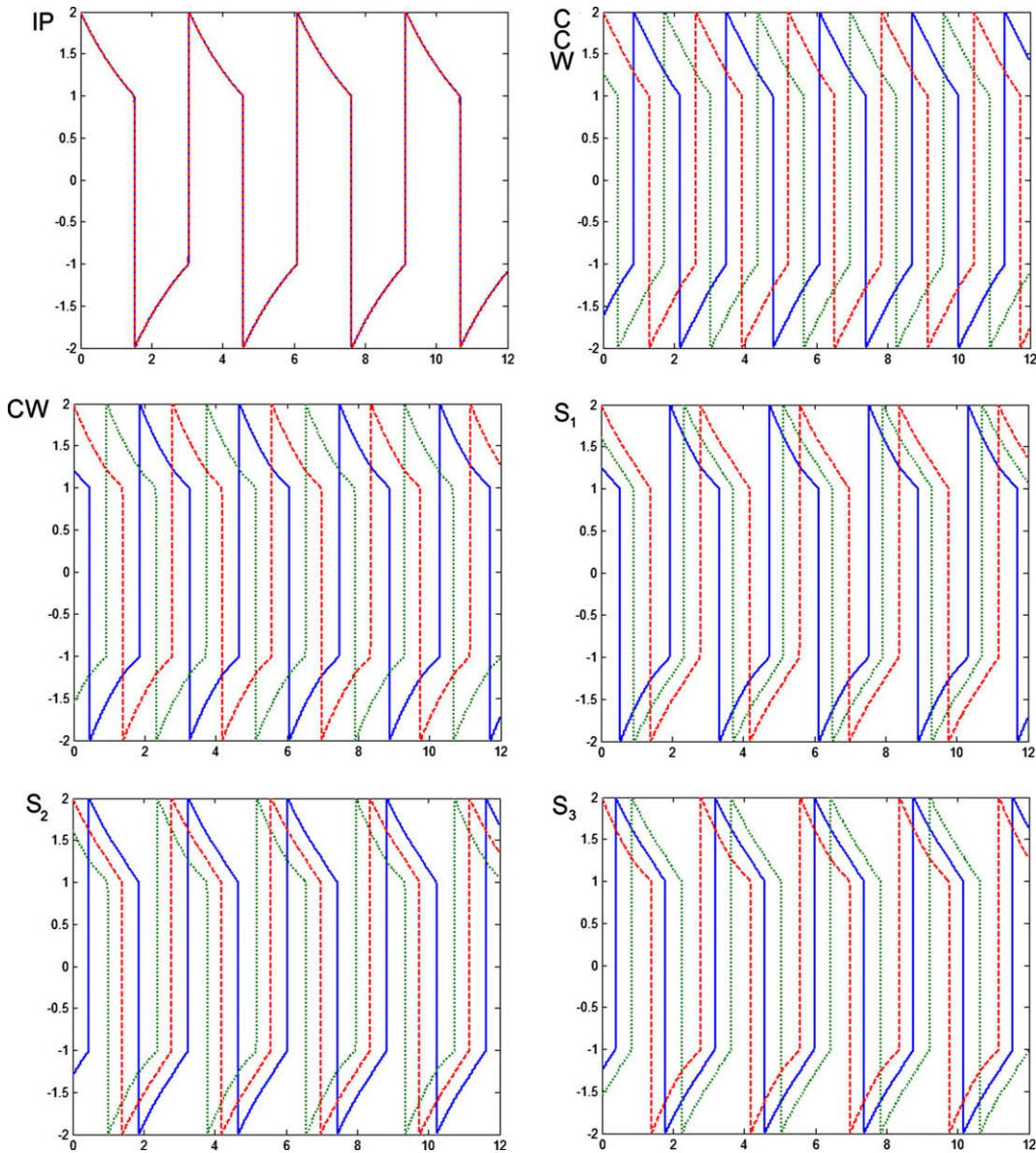


Fig. 3. Schematic diagram of model of relaxation oscillator. Single arrows indicate slow segments of the limit cycle while double arrows indicate rapid flow which is modeled as an instantaneous jump. We omit the region of phase space which lies between  $x = -1$  and  $x = 1$ .

- S<sub>1</sub> clockwise mode with unevenly spaced jumps ordered x–y–z
- S<sub>2</sub> clockwise mode with unevenly spaced jumps ordered y–z–x
- S<sub>3</sub> clockwise mode with unevenly spaced jumps ordered z–x–y

Regarding the stability of these periodic solutions, for  $\alpha > 0$  we find that the clockwise modes, CW, S<sub>1</sub>, S<sub>2</sub> and S<sub>3</sub>, are always unstable (when they exist). (We were able to obtain plots of these motions even though they are unstable by knowing their initial conditions, obtained in a manner to be explained later.)

With two stable steady states, IP and CCW, the question arises as to which initial conditions lie in the basin of attraction of each of these modes. This requires that we define the “jump-from” cube, defined by  $|x| = 1, |y| = 1, |z| = 1$ , which lies inside the “jump-to” cube defined by  $|x| = 2, |y| = 2, |z| = 2$ . We choose to represent an initial condition by a point on the  $z = 2$  face of the jump-to cube, i.e. by the parameters  $(x_0, y_0)$ , where  $x(0) = x_0, y(0) = y_0$  and  $z(0) = 2$ . This can be done without loss of generality because Eqs. (5)–(7) are invariant under cyclic permutation. That is, if we identify a point on the jump-to cube with its asymptotic behavior, then all six faces will be geometrically congruent. Thus Fig. 5 shows the asymptotic



**Fig. 4.** Six different periodic motions obtained by numerically integrating Eqs. (5)–(7) for  $\alpha = 0.1$ . The solid, dotted and dashed lines respectively correspond to the x, y and z coordinates. The initial conditions are: IP = (2, 2, 2), CCW = (−1.6336, 1.2783, 2), CW = (1.2137, −1.5583, 2), S<sub>1</sub> = (1.2653, 1.6165, 2), S<sub>2</sub> = (−1.3061, 1.6232, 2), S<sub>3</sub> = (−1.2546, −1.5516, 2).

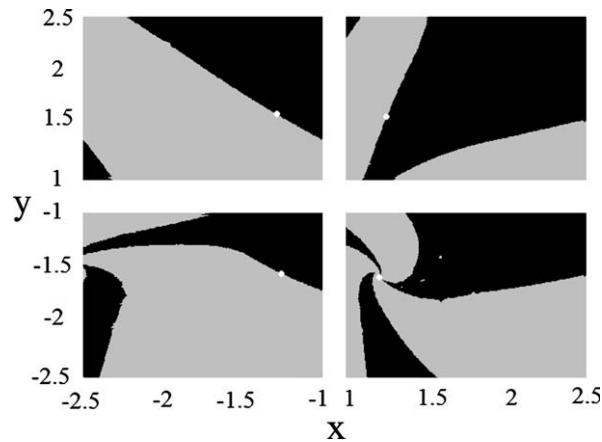


**Fig. 5.** Asymptotic behavior of a field of initial conditions  $x(0) = x_0, y(0) = y_0$  lying in the plane  $z(0) = 2$  for  $\alpha = 0.1$ . Black region represents initial conditions which approach the IP mode while gray region represents initial conditions which approach the CCW mode. White region represents initial values  $|x_0| < 1$  and  $|y_0| < 1$  which are omitted, see text. White dots represent the unstable periodic motions CW,  $S_1, S_2$  and  $S_3$ , cf. Fig. 4.

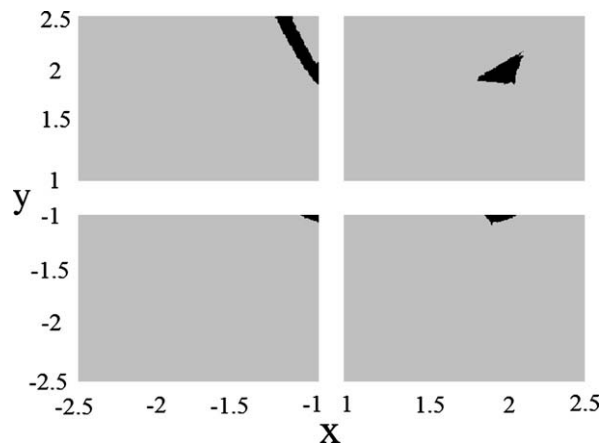


**Fig. 6.** Asymptotic behavior of a field of initial conditions  $x(0) = x_0, y(0) = y_0$  lying in the plane  $z(0) = 2$  for  $\alpha = 0.653$ . Black region represents initial conditions which approach the IP mode while gray region represents initial conditions which approach the CCW mode. White region represents initial values  $|x_0| < 1$  and  $|y_0| < 1$  which are omitted, see text. Comparable plots for larger values of  $\alpha$  show no black region indicating that a bifurcation involving a change in stability of the IP mode occurs for  $\alpha \approx 0.653$ .

behavior of a field of initial conditions lying in the plane  $z(0) = 2$  for  $\alpha = 0.1$ . Note that initial values  $|x_0| < 1$  and  $|y_0| < 1$  are omitted as stated above. For comparison, Fig. 6 shows the corresponding diagram for  $\alpha = 0.653$ . For values of  $\alpha > 0.653$  the corresponding figure shows that the only stable mode is CCW. Evidently a bifurcation has taken place for  $\alpha \approx 0.653$  in which the IP mode has become unstable.

In order to study the existence and stability of these various periodic motions, we turn to an analytic approach.

**4. Analytic approach**

To begin the analysis we consider the dynamics of the uncoupled ( $\alpha = 0$ ) system. Eq. (5) reduces to:

$$\frac{dx}{dt} + \frac{1}{2}x = 0 \tag{11}$$

with similar equations for  $y$  and  $z$ . The solution to this equation is

$$x(t) = x(0)e^{-t/2} \text{ for } |x| > 1 \text{ with a jump at } x = \pm 1 \tag{12}$$

The solutions correspond to straight lines in  $x$ - $y$ - $z$  phase space which pass through the origin when extended. However, each time a coordinate reaches  $\pm 1$ , the oscillator jumps and consequently moves onto a different one of these lines.

As in the previous section, we will consider the fate of orbits which begin on the  $z = 2$  face. For an orbit beginning at coordinates  $(x_0, y_0, 2)$  with  $|x_0| < |y_0| < 2$ , the  $x$ -coordinate will reach  $\pm 1$  first, and the orbit will proceed with clockwise jumps. If on

the other hand,  $|y_0| < |x_0| < 2$ , the  $y$ -coordinate will reach  $\pm 1$  first, and the orbit will proceed with counter-clockwise jumps. Every motion that begins outside the jump-to cube of size 2 will approach the cube and eventually all values of  $|x|$ ,  $|y|$  and  $|z|$  will remain  $\leq 2$ , becoming a periodic motion of period  $4 \log 2$ .

The  $\alpha = 0$  case just discussed is highly degenerate. Consequently, our next step is to determine which periodic orbits persist for non-zero  $\alpha$ . The general solution to Eqs. (8)–(10) is given by:

$$x(t) = \frac{2}{3} e^{-\beta_1 t} \left( x_0 \cos(\gamma t) + y_0 \sin \left( \gamma t + \frac{7\pi}{6} \right) + z_0 \sin \left( \gamma t - \frac{\pi}{6} \right) \right) + \frac{1}{3} e^{-\beta_2 t} (x_0 + y_0 + z_0) \tag{13}$$

where

$$\beta_1 = \frac{2 - \alpha}{4(\alpha^2 - \alpha + 1)} \tag{14}$$

$$\beta_2 = \frac{1}{2(1 + \alpha)} \tag{15}$$

$$\gamma = \frac{\sqrt{3}\alpha}{4(\alpha^2 - \alpha + 1)} \tag{16}$$

Expressions for  $y(t)$  and  $z(t)$  are given by cyclic permutations of Eq. (13). The  $\beta_i$  terms indicate whether the solution will grow or decay with time. For positive  $\alpha$ , the  $\beta_2$  is always positive, therefore the second term in the solution is always decaying. However,  $\beta_1$  has a transition at  $\alpha = 2$ ; for  $0 < \alpha < 2$  there is always exponential decay while for  $\alpha > 2$  there is exponential growth.

An exact solution for the IP mode with  $x(t) = y(t) = z(t)$  can be determined analytically, since, for this special case, Eqs. (5)–(7) reduce to:

$$\dot{x} = -\frac{1}{2(1 + \alpha)} x \tag{17}$$

which we can easily integrate to obtain the solution:

$$x(t) = y(t) = z(t) = \pm x_0 \exp \left( -\frac{t}{2(1 + \alpha)} \right) \tag{18}$$

This results in exponential decay for all values of  $\alpha > -1$ . A motion which initially begins at  $(2, 2, 2)$  will arrive at  $(1, 1, 1)$  at time  $2(1 + \alpha) \log 2$ . It then jumps to  $-2$  and repeats the process. Hence the period of the IP mode is  $4(1 + \alpha) \log 2$ . For  $\alpha < -1$ , the system experiences exponential growth; since the oscillation has a constantly increasing amplitude, it will never reach 1 and so there is no longer a limit cycle associated with the motion.

A semi-analytical solution for CCW mode can be obtained by using the closed form solution (13) and its cyclic permutations together with the initial conditions  $(x(0), y(0), 2)$ . This solution is valid until a time, call it  $t = t_1$ , at which  $y$  first jumps, i.e.  $y(t_1) = 1$ . This is then followed by another application of the closed form solution (13), this time with initial conditions  $(x(t_1), -2, z(t_1))$ . Note that although  $y$  has jumped from 1 to  $-2$ ,  $x$  and  $z$  maintain the same values they had before the jump in  $y$ . This process is then continued until  $x$  jumps from 1 to  $-2$ , then  $y$ ,  $x$  and  $z$  each jump from  $-1$  to 2, completing the CCW periodic motion. However, we can take a short cut based on the symmetry of the system and obtain the following conditions for the CCW mode:

$$\text{CCW mode: } z(0) = 2 \quad y(t_1) = 1, \quad x(t_1) = -y(0), \quad z(t_1) = -x(0) \tag{19}$$

which represent three nonlinear algebraic equations for the three unknowns  $t_1$ ,  $x(0)$  and  $y(0)$ . The period of the CCW mode is  $T = 6t_1$ , e.g. for  $\alpha = 0.1$  and  $\alpha = 1$  we find:

$$\text{CCW mode: } \alpha = 0.1, \quad T = 2.6100, \quad x(0) = -1.6336, \quad y(0) = 1.2783 \tag{20}$$

$$\alpha = 1, \quad T = 3.4608, \quad x(0) = -2.1831, \quad y(0) = 1.7901 \tag{21}$$

The CW mode can be treated in the same way by interchanging the roles of  $x$  and  $y$ . The conditions for the CW mode become:

$$\text{CW mode: } z(0) = 2 \quad x(t_1) = 1, \quad y(t_1) = -x(0), \quad z(t_1) = -y(0) \tag{22}$$

For  $\alpha = 1$  no solution was obtained, implying that the CW mode does not exist for  $\alpha = 1$ . For  $\alpha = 0.1$  we find:

$$\text{CW mode: } \alpha = 0.1, \quad T = 2.7948, \quad x(0) = 1.2137, \quad y(0) = -1.5583 \tag{23}$$

$$\alpha = 1, \quad \text{does not exist} \tag{24}$$

In the case of the unevenly spaced clockwise modes  $S_1$ ,  $S_2$  and  $S_3$ , a similar semi-analytical approach may be used, but will involve three times  $t_1$ ,  $t_2$  and  $t_3$  representing the time between jumps, cf. Fig. 4. The period of the  $S_i$  modes is  $T = 2(t_1 + t_2 + t_3)$ . We again find that these modes do not exist for  $\alpha = 1$ . The values for  $\alpha = 0.1$  are found as follows:

$$S_1 \text{ mode: } \alpha = 0.1, \quad T = 2.8014, \quad x(0) = 1.2653, \quad y(0) = 1.6165 \tag{25}$$

$$\alpha = 1, \quad \text{does not exist} \tag{26}$$

$$S_2 \text{ mode: } \alpha = 0.1, \quad T = 2.8014, \quad x(0) = -1.3061, \quad y(0) = 1.6232 \tag{27}$$

$$\alpha = 1, \quad \text{does not exist} \tag{28}$$

$$S_3 \text{ mode: } \alpha = 0.1, \quad T = 2.8014, \quad x(0) = -1.2546, \quad y(0) = -1.5516 \tag{29}$$

$$\alpha = 1, \quad \text{does not exist} \tag{30}$$

Using the foregoing semi-analytical approach, we were able to plot the period of each of the six modes as a function of the coupling parameter  $\alpha$ . See Fig. 7. In order to better understand the bifurcations which appear in Fig. 7, we next consider the stability of these modes.

#### 4.1. Stability

The stability of the various periodic motions may be determined by numerically integrating Eqs. (8)–(10), starting with initial conditions close to those given by the semi-analytic approach. In this way we obtain the result that for  $\alpha > 0$  the CCW mode is always stable, and the CW mode and the  $S_i$  modes are always unstable. The IP mode changes stability at  $\alpha \approx 0.653$ . From Fig. 7 we see that the latter change in stability is accompanied by a pitchfork bifurcation in which the three  $S_i$  modes merge with the IP mode.

Stability may also be determined by using a variant of the foregoing semi-analytical approach. Let the periodic motion be defined by the initial condition  $(x_0, y_0, 2)$ . This initial condition will lead to a sequence of jumps which will eventually return to the same initial state. The idea of the stability analysis is to replace the initial condition with  $(x_0 + u, y_0 + v, 2)$ , where  $u$  and  $v$  represent small deviations from the periodic solution. This new initial condition will cause a change in the time of the first jump from  $t_1$  to say  $t_1 + w$ , where  $w$  will be a function of  $u$  and  $v$ . If, for the sake of argument, we suppose that the first jump was in  $x$ , then at time  $t_1 + w$ ,  $x$  will equal 1 while  $y$  and  $z$  will take on values which differ slightly from the original values associated with the periodic motion. These deviations in  $y$  and  $z$  will be functions of  $u$  and  $v$ . Proceeding in this way we will see a sequence of jumps, each occurring at a slightly different time than that of the original jump, and each occurring at a slightly different point in phase space. After the last jump, where the original periodic motion returns to its initial state, we end up at a point which may be written in the form  $(x_0 + F(u, v), y_0 + G(u, v), 2)$ . Thus this procedure sets up a map from  $(u, v)$  to  $(F(u, v), G(u, v))$ , the linearization of which governs the stability of the original periodic motion. The condition for stability is that the modulus of both eigenvalues of the linearized map be less than unity. This approach to stability is particularly useful when used with perturbation expansions, described next.

#### 4.2. Perturbation results

Although an exact solution to the model Eqs. (8)–(10) is available between jumps, cf. Eq. (13), an exact solution cannot be found for the periodic motions CCW, CW and  $S_i$  because these involve solving a transcendental equation for the time at which each of the jumps occurs. Nevertheless we may obtain closed form approximate expressions for these motions, as well as determinations of the stability of all the periodic motions, by using regular perturbations valid for small values of  $\alpha$ .

For small  $\alpha$ , Eq. (13) reduces to:

$$x(t) = \left( x_0 + \alpha t \frac{z_0}{2} + \alpha^2 \frac{y_0}{8} (t^2 - 4t) \right) e^{-\frac{t}{2}} + O(\alpha^3) \tag{31}$$

Similar expressions for  $y(t)$  and  $z(t)$  are given by cyclic permutations of this equation.

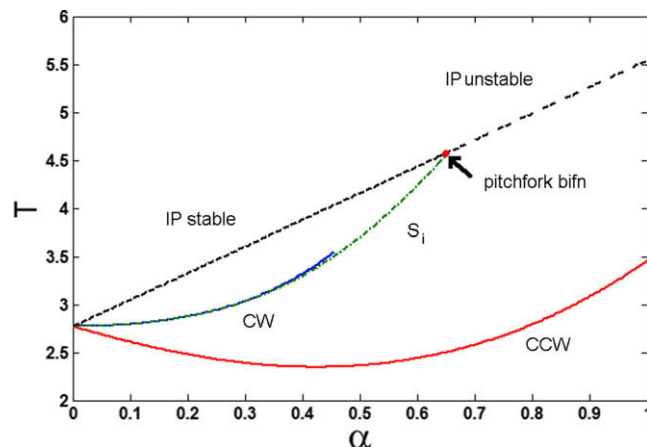


**Fig. 7.** Variation of the periods  $T$  of the various limit cycles as the coupling parameter,  $\alpha$ , changes.

### 4.3. CCW mode

We have seen that the conditions for the CCW mode are given by Eq. (19), which we repeat here for the convenience of the reader:

$$\text{CCW mode: } z_0 = 2 \quad y(t_1) = 1, \quad x(t_1) = -y_0, \quad z(t_1) = -x_0 \tag{32}$$

in which  $x(t)$ ,  $y(t)$  and  $z(t)$  are now given by the truncated expression (31) and its cyclic permutations. We expand

$$x_0 = \xi_0 + \alpha \xi_1 + \alpha^2 \xi_2 + O(\alpha^3) \tag{33}$$

$$y_0 = \eta_0 + \alpha \eta_1 + \alpha^2 \eta_2 + O(\alpha^3) \tag{34}$$

$$t_1 = \tau_0 + \alpha \tau_1 + \alpha^2 \tau_2 + O(\alpha^3) \tag{35}$$

and substitute (33)–(35) into (32). Collecting terms and solving for the  $\xi_i$ ,  $\eta_i$  and  $\tau_i$ , we obtain:

$$x_0 = -2^{2/3} - \frac{2\alpha}{3} \log 2 - 2^{1/3}(\log 2)^2 \frac{\alpha^2}{9} + O(\alpha^3) \tag{36}$$

$$y_0 = 2^{1/3} + 2^{2/3} \frac{\alpha}{6} \log 2 + \frac{\alpha^2}{18} \log 2(2 \log 2 + 9) + O(\alpha^3) \tag{37}$$

$$t_1 = \frac{2}{3} \log 2 - \frac{2^{1/3} \log 2}{3} \alpha - \frac{\alpha^2}{36} 2^{2/3} \log 2(\log 2 - 6) + O(\alpha^3) \tag{38}$$

For  $\alpha = 0.1$ , the values (36), and (37) of  $(x_0, y_0, z_0)$  obtained using the perturbation technique are  $(-1.6343, 1.2861, 2)$ , in good agreement with the numerically generated values (20), which were  $(-1.6336, 1.2783, 2)$ .

Using the method described in the previous section on Stability, we find that the eigenvalues for the CCW mode are

$$1 + \frac{2^{1/3}(3 \log 2 - 9)\alpha}{2} \pm i \frac{2^{1/3}(\sqrt{3} \log 2 - 3\sqrt{3})\alpha}{2} + O(\alpha^2) \tag{39}$$

which have modulus

$$1 + \frac{(3 \log 2 - 9)\sqrt[3]{2}\alpha}{2} + O(\alpha^2) \approx 1 - 4.35968 \alpha < 1 \quad \text{for } \alpha > 0 \tag{40}$$

which shows that the CCW mode is a stable spiral (a sink) for small  $\alpha$ .

### 4.4. CW mode

Proceeding in the same fashion, we find the following results for the CW mode:

$$x_0 = 2^{1/3} - \frac{2\alpha}{3} \log 2 + 2^{2/3} \log 2 \frac{\alpha^2}{12} (\log 2 - 2) + O(\alpha^3) \tag{41}$$

$$y_0 = -2^{2/3} + 2^{1/3} \frac{\alpha}{3} \log 2 - \frac{\alpha^2}{9} \log 2(\log 2 - 6) + O(\alpha^3) \tag{42}$$

$$t_1 = \frac{2}{3} \log 2 + \frac{\alpha^2}{18} 2^{1/3} \log 2(\log 2 + 6) + O(\alpha^3) \tag{43}$$

For  $\alpha = 0.1$ , the values (41), and (42) of  $(x_0, y_0, z_0)$  obtained using the perturbation technique are  $(1.2125, -1.5542, 2)$ , in good agreement with the numerically generated values (23), which were  $(1.2137, -1.5583, 2)$ .

Using the method described in the previous section on Stability, we find that the eigenvalues for the CW mode are approximately

$$1 + 7.1433\alpha \pm i4.1242\alpha + O(\alpha^2) \tag{44}$$

which have modulus  $1 + 7.1433\alpha + O(\alpha^2) > 1$  for  $\alpha > 0$ , showing that the CW mode is an unstable spiral (a source) for small  $\alpha$ .

### 4.5. Stability of the IP mode

Using the method described in the previous section on Stability, the linearized map obtained for the IP mode is:

$$\begin{bmatrix} 1 + (3 - 2 \log 2)\alpha - \frac{64 \log 2 + 75}{2} \alpha^2 & -(2 \log 2 + 6)\alpha + \frac{12 \log^2 2 + 37 \log 2 + 75}{2} \alpha^2 \\ (2 \log 2 + 6)\alpha - \frac{12 \log^2 2 + 55 \log 2 + 75}{2} \alpha^2 & 1 - (12 + 4 \log 2)\alpha + (6 \log^2 2 + 34 \log 2 + 66)\alpha^2 \end{bmatrix} \tag{45}$$

from which the eigenvalues are approximately:

$$\lambda_1 = 1 - 10.125\alpha + O(\alpha^2) \text{ and } \lambda_2 = 1 - 3.034\alpha + O(\alpha^2) \tag{46}$$

Since both of these eigenvalues are real and less than unity for small  $\alpha > 0$ , the IP mode is a stable node.

#### 4.6. $S_1, S_2$ and $S_3$

The same perturbation procedure which was used on the CCW and CW modes may also be used on the  $S_i$  modes, which are clockwise periodic motions with unevenly spaced jumps. Table 1 shows the initial condition coordinates for these periodic motions and the associated times between jumps. Note that these times are cyclic permutations of each other, so the period  $T$  of each of these motions is the same and equals

$$T = 2(t_1 + t_2 + t_3) = 4 \log 2 + O(\alpha^2) \approx 2.7726 \tag{47}$$

which compares well with the numerically obtained value of 2.8014, cf. Eq. (25).

To determine the stability of these motions, the method described in the previous section on Stability was used and yielded the same eigenvalues for each of the  $S_i$  modes:

$$\lambda_1 = 1 + 2.943\alpha + O(\alpha^2), \quad \lambda_2 = 1 - 7.705\alpha + O(\alpha^2) \tag{48}$$

Both eigenvalues are real, and one is larger than unity, while the other is smaller than unity. Each limit cycle is therefore a saddle.

#### 4.7. Global bifurcations

As discussed in Eqs. (11), and (12),  $\alpha = 0$  is a very degenerate parameter value. At this value, all the orbits are periodic. Upon changing  $\alpha$  from its zero value, only six limit cycles persist: IP, CCW, CW,  $S_1, S_2, S_3$ . As  $\alpha$  passes through zero, there is an exchange of stability type between the CCW and the CW modes. The IP mode also changes its stability from that of an unstable node to a stable node. However, the  $S_i$  still persist as saddles.

As  $\alpha$  is further increased, a variety of bifurcations occur, see Fig. 7. At  $\alpha = 0.653$ , the IP and the  $S_i$  limit cycles merge. The  $S_i$  disappear and the IP changes from a stable node to a saddle in a pitchfork bifurcation. The two other limit cycles (the CW and CCW) also undergo their own bifurcations. At  $\alpha = 0.459$  the CW mode moves to the edge of the admissible zone and “falls off” into the forbidden region. That is, the initial conditions which give rise to the CW mode lie inside the jump-from cube of size 1. (Recall that we have omitted initial conditions inside this cube because in the case of the uncoupled oscillator they do not approach the stable limit cycle.) As for the CCW mode, its amplitude tends to infinity as  $\alpha$  approaches 2, and so it does not exist for  $\alpha > 2$ . For values of  $\alpha$  which are greater than 2 the only periodic motion is the IP mode, which is unstable: all motions except for a set of measure zero escape to infinity. Fig. 8 shows the location of each periodic motion as a point on the  $z = 2$  face of the jump-to cube, for varying  $\alpha$ , cf. Fig. 5.

**Table 1**

The initial condition coordinates for  $z(0) = 2$ , and the time between jumps, for the saddles,  $S_i, i = 1, 2, 3$  for small coupling  $\alpha$

$x_0$ Coordinate	$y_0$ Coordinate	Time between jumps
$S_1 : 2^{1/3} + \frac{\alpha}{9}(\log 2)^2$	$2^{2/3} + \alpha \frac{2^{1/3}}{3} \log 2$	$t_1 = 2 \log 2/3 + \alpha \frac{2^{2/3}}{9} ((\log 2)^2 + 6 \log 2)$
		$t_2 = 2 \log 2/3 - \alpha \frac{2^{2/3}}{9} ((\log 2)^2 + 6 \log 2)$
		$t_3 = 2 \log 2/3$
$S_2 : -2^{1/3} - \frac{2\alpha}{3} \log 2$	$2^{2/3} + \alpha \frac{2^{1/3}}{9} (3 \log 2 + (\log 2)^2)$	$t_1 = 2 \log 2/3$
		$t_2 = 2 \log 2/3 + \alpha \frac{2^{2/3}}{9} ((\log 2)^2 + 6 \log 2)$
		$t_3 = 2 \log 2/3 - \alpha \frac{2^{2/3}}{9} ((\log 2)^2 + 6 \log 2)$
$S_3 : -2^{1/3} + \frac{\alpha}{9}(\log 2)^2$	$-2^{2/3} + \alpha \frac{2^{1/3}}{9} (3 \log 2 + (\log 2)^2)$	$t_1 = 2 \log 2/3 - \alpha \frac{2^{2/3}}{9} ((\log 2)^2 + 6 \log 2)$
		$t_2 = 2 \log 2/3$
		$t_3 = 2 \log 2/3 + \alpha \frac{2^{2/3}}{9} ((\log 2)^2 + 6 \log 2)$

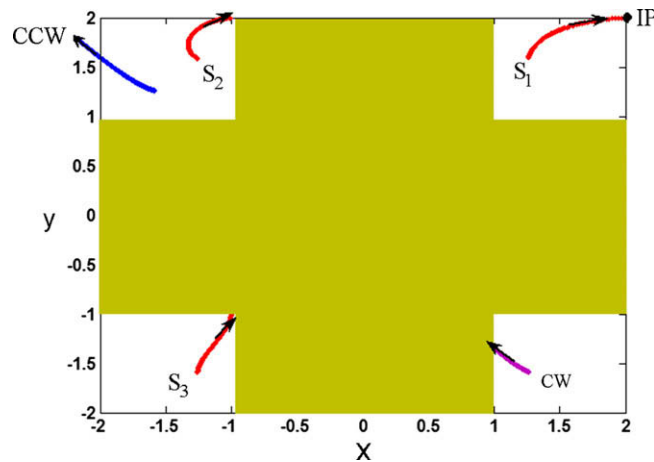


**Fig. 8.** Location of the various periodic motions as points on the  $z = 2$  face of the jump-to-cube, as the coupling parameter  $\alpha$  changes. The saddle-like  $S_2$  modes merge with the IP mode at  $\alpha \approx 0.653$ . Note that at this value,  $S_2$  and  $S_3$  approach  $(-1, 2)$  and  $(-1, -1)$  respectively, on the jump-from cube of size 1, both of which are immediately mapped to  $(2, 2)$  of the jump-to-cube i.e. to the IP mode. The CW mode enters the interior of the jump-from cube of size 1 at  $\alpha \approx 0.459$ . The CCW mode moves out towards infinity as  $\alpha$  approaches 2.

## 5. Conclusion

In this work we have investigated the dynamics of a ring of three identical relaxation oscillators using a model which involves jumps. We have found that the system exhibits wave-like motions (CCW, CW and  $S_i$  modes) as well as synchrony (IP mode). The model involves a single parameter,  $\alpha$ , which represents the strength of inhibitory coupling. As  $\alpha$  is changed a variety of bifurcations occur in which some periodic motions disappear and others change their stability. In particular we find that in the range  $0 < \alpha < 0.653$  there are two stable modes, IP and CCW. This means that the system can function as a decision-making device by sorting initial conditions according to their steady state.

The dynamics observed in this system may be compared to results reported in a related work [6] which dealt with a ring of three sinusoidal (versus relaxation) oscillators. In that case both the CW and CCW modes were stable for all  $\alpha > 0$ , but the IP mode was either unstable or didn't exist. This suggests that as  $\epsilon$  changes in a system of van der Pol oscillators, from small values corresponding to sinusoidal oscillations to large values corresponding to relaxation oscillations, a series of bifurcations occurs which involves changes of stability between IP and CW modes. In the case of two coupled van der Pol oscillators, such bifurcations due to a change in  $\epsilon$  between IP and OP (out-of-phase) modes have been reported [17].

Extensions of the present work could include (i) breaking the symmetry of the model by making either the individual oscillators non-identical, or by having non-identical coupling parameters, or (ii) increasing the number of oscillators in the ring while keeping the symmetry fixed.

## Acknowledgements

Authors JB and SS gratefully acknowledge the hospitality of the Department of Theoretical and Applied Mechanics, Cornell University. Support received from the Moroccan American Commission for Educational and Cultural Exchange through the Fulbright Program is gratefully acknowledged by author SS. This work was partially supported under the CMS NSF Grant CMS-0600174 "Nonlinear Dynamics of Coupled MEMS Oscillators".

## References

- [1] Hoppensteadt F, Izhikevich E. Oscillatory neurocomputers with dynamic connectivity. *Phys Rev Lett* 1999;82:2983–6.
- [2] Zhalalutdinov MK, Baldwin JW, Marcus MH, Reichenbach RB, Parpia JM, Houston BH. Two-dimensional array of coupled nanomechanical resonators. *Appl Phys Lett* 2006;88:143504.
- [3] Rand R, Wong J. Dynamics of four coupled phase-only oscillators. *Commun Nonlinear Sci Numer Simul* 2008;13:501–7.
- [4] Cohen AH, Holmes PJ, Rand RH. The nature of the coupling between segmental oscillators of the Lamprey spinal generator for locomotion: a mathematical model. *J Math Biol* 1982;13:345–69.
- [5] van der Pol B. On relaxation oscillations. *Philos Mag* 1926;2:978–92.
- [6] Mendelowitz L, Verdugo A, Rand R. Dynamics of three coupled limit cycle oscillators with application to artificial intelligence. *Commun Nonlinear Sci Numer Simul* 2009;14(4):270–83.
- [7] Rand RH. *Lect Note Nonlinear Vib*, ver. 52; 2005. Available on-line at <<http://audiophile.tam.cornell.edu/randdocs/nlvibe52.pdf>>.
- [8] Cole JD. *Perturbation methods in applied mathematics*. Blaisdell Pub. Co.; 1968.
- [9] Storti D, Rand RH. Dynamics of two strongly coupled relaxation oscillators. *SIAM J Appl Math* 1986;46:56–67.
- [10] Storti D, Rand RH. A simplified model of coupled relaxation oscillators. *Int J Nonlinear Mech* 1987;22:283–9.
- [11] Storti D, Rand RH. Subharmonic entrainment of a forced relaxation oscillator. *Int J Nonlinear Mech* 1988;23:231–9.
- [12] Levi M. A period-adding phenomenon. *SIAM J Appl Math* 1990;50:943–55.

- [13] Guckenheimer J, Wechselberger M, Young LS. Chaotic attractors of relaxation oscillators. *Nonlinearity* 2006;19:701–20.
- [14] Somers D, Kopell N. Rapid synchronization through fast threshold modulation. *Biol Cybernetics* 1993;68:393–407.
- [15] Somers D, Kopell N. Waves and synchrony in networks of oscillators of relaxation and non-relaxation type. *Physica D* 1995;89:169–83.
- [16] Izhikevich EM. Phase equations for relaxation oscillators. *SIAM J Appl Math* 2000;60:1789–804.
- [17] Storti DW, Reinhall PG. Stability of in-phase and out-of-phase modes for a pair of linearly coupled van der Pol oscillators. In: Guran A, editor. *Nonlinear dynamics: The Richard Rand 50th anniversary volume*. World Scientific; 1997. p. 1–23. [Chapter 1].